Radiation Effects & Defects in Solids
Vol. 164, Nos. 5–6, May–June 2009, 357–362

Charged particle detection at GRAAL

F. Mammoliti[a,b]*, V. Bellini[a,b], A. Giusa[a,b], C. Randieri[a,b], G. Russo[a,b], M.L. Sperduto[a,b], M.C. Sutera[b], A. D'Angelo[c,d], R. Di Salvo[d], A. Fantini[c,d], D. Franco[c,d], D. Moricciani[d], C. Schaerf[c,d], V. Vegna[c,d], P. Levi Sandri[e], G. Mandaglio[b,f] and G. Giardina[b,f]

[a]*Dipartimento di Fisica ed Astronomia, Università di Catania, via Santa Sofia 64, I-95123 Catania, Italy;* [b]*INFN – Sezione di Catania, via Santa Sofia 64, I-95123 Catania, Italy;* [c]*Dipartimento di Fisica, Università di Roma Tor Vergata, via della Ricerca Scientifica 1, I-00133 Roma, Italy;* [d]*INFN – Sezione di Roma Tor Vergata, via della Ricerca Scientifica 1, I-00133 Roma, Italy;* [e]*INFN – Laboratori Nazionali di Frascati, via Enrico Fermi 40, I-00044 Frascati, Italy;* [f]*Dipartimento di Fisica, Università di Messina, Salita Sperone 31, I-98166 Messina, Italy*

(*Received 24 May 2008; final version received 8 February 2009*)

Experimental results on proton and charged pion detection obtained from a study of the $\gamma + \mathrm{n} \rightarrow \mathrm{p} + \pi^-$ reaction are reported in detail. Data have been collected using the tagged and linearly polarized photon beam, impinging on a deuterium target, and the large solid angle apparatus of the GRAAL facility in Grenoble (France). The energy of the charged particles was measured using a BGO calorimeter. A comparison of the experimental data with a GEANT3-based simulation is also presented.

Keywords: photonuclear reaction; SRIM simulation; BGO calorimeter; deuterium target; $\gamma + \mathrm{n} \rightarrow \mathrm{p} + \pi^-$ channel reaction; Fermi momentum

1. Introduction

The GRAAL collaboration is engaged in the study of meson photoproduction on protons and neutrons with the use of liquid hydrogen and deuterium targets (*1*). Simultaneous detection of the produced particles is required in such experiments. We investigated the $\gamma + \mathrm{d} \rightarrow \mathrm{p} + \pi^- + (\mathrm{p})$ reaction, in which the neutron, in the deuteron, is considered as the participant and the proton as the spectator particle, respectively. Deuterium is the simplest system in nature containing a neutron; moreover this neutron is only weakly bound inside the nucleus, allowing for an evaluation of the Fermi momentum. The final state of the reaction contains two different particles detected simultaneously by the central experimental setup. An experimental problem arises whenever the BGO calorimeter is not able to stop fast charged particles, and so a direct measure of the total energy is not always possible. This work is organized as follows: first, the experimental setup is described, then the measurement results are shown. In particular, we present a Monte Carlo simulation of proton detection in the BGO performed with the software SRIM (2), the

*Corresponding author. Email: francesco.mammoliti@ct.infn.it

ISSN 1042-0150 print/ISSN 1029-4953 online

DOI: 10.1080/10420150902811698
http://www.informaworld.com

graphical and kinematical methods of selection and finally a comparison between the measured and simulated energy for the charged particles.

2. Experimental setup

The experiment has been carried out with the GRAAL apparatus (*3*), installed at the European Synchrotron Radiation Facility in Grenoble (France). Data have been collected with a tagged and linearly polarized photon beam, operating in the energy range from 0.7 up to 1.5 GeV (*4*), produced by the Compton backscattering of laser light on the 6.04 GeV electrons circulating in the storage ring, and the large solid angle experimental setup of the GRAAL facility. The tagging detector, constituted by scintillators and Si microstrips (providing time and energy, respectively), provides an uniform energy resolution of 16 MeV (FWHM), which corresponds to a relative error of 1.1% at the maximum energy.

The GRAAL detection system (LAGRANγE detector, Figure 1) covers almost the whole solid angle and includes two main parts. The forward part, in the angular range $\theta \leq 25°$, consists of two planar wire chambers for the tracking of charged particles, two walls of plastic scintillators (26 horizontal and 26 vertical bars placed at 3 m from the target), designed for TOF, dE/dx, and angular measurements of charged particles, and a shower detector (16 vertical modules made of lead and plastic scintillator) that provides TOF and angular measurements of both neutral and charged particles (*3*, *5*). The central part, covering the angular range $25° \leq \theta \leq 155°$, consists of two cylindrical wire chambers for tracking the charged particles, a barrel detector (made of 32 5 mm thick plastic scintillator bars) for measuring dE/dx of charged particles, and an electromagnetic calorimeter (called BGO) (6–8) made of 480 $Bi_4Ge_3O_{12}$ crystals (15 rings and 32 sectors), designed to measure energies and angles for gammas and low-energy protons as well as the angles for charged pions and neutrons (*9*).

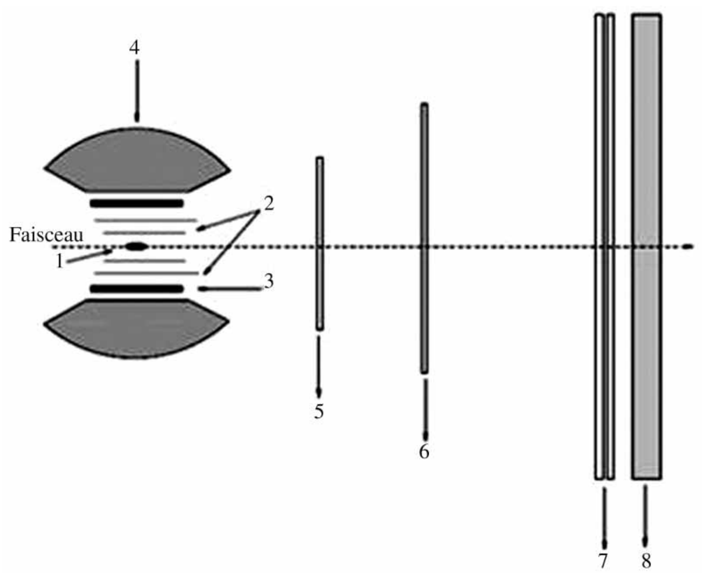

Figure 1. Schematic view of the Lagrange detector: 1, target; 2, cylindrical wire chambers; 3, barrel of scintillators; 4, BGO calorimeter; 5 and 6, planar wire chambers; 7, walls of plastic scintillators; 8, shower wall.

3. Results

In this study, the events have been selected among those detected in the central region of the GRAAL apparatus. The reaction $\gamma + \mathrm{n} + (\mathrm{p}) \rightarrow \mathrm{p} + \pi^- + (\mathrm{p})$ was chosen because of its large cross-section; moreover, the two-body kinematics provide a clear separation between events in the BGO calorimeter induced by protons and charged pions coming from competitive channels. If fully detected in the central part of the apparatus, the final state of the reaction appears as two clusters in the BGO calorimeter, corresponding to p and π^-. A cluster is defined as a group of adjacent cells in which energy is deposited. Each cluster is associated with a single interacting particle (*6*); moreover, a cluster is associated to a charged particle if there are signals both in the barrel and in the cylindrical chambers geometrically associated with this cluster. The GRAAL apparatus has been simulated in a Monte Carlo program that is based on a GEANT3 code (*10*) from the CERN libraries. It works together with an event generator, which produces all interesting photoproduction reactions on the proton and on the neutron bound in the deuteron. Simulating the reaction $\gamma + \mathrm{n} + (\mathrm{p}) \rightarrow \mathrm{p} + \pi^- + (\mathrm{p})$, the energy of the charged photoproduced particle was obtained. In particular, we have found that, also with the maximum beam energy of 1.5 GeV, the energy of the proton is lower than 470 MeV, according to the solid angle covered by the BGO calorimeter.

We have performed a Monte Carlo simulation of proton detection in the BGO by using the software SRIM. In Figure 2, the output of a simulation, when the energy of the proton is 450 MeV, is reported. Red lines represent the path of the proton, while the black points are the stopping positions (color online). The energy of protons varied from 300 to 530 MeV (Table 1). All protons with energy lower than 480 MeV are stopped, whereas protons with energy above 500 MeV are almost totally transmitted. This result is supported by the GEANT simulation output, allowing us to rely on a complete identification of protons in the final state of the studied reaction.

In order to identify the particles produced in the reaction, we have performed both a graphical preselection and a kinematical selection of the events. Figure 3 shows the energy lost in the barrel detector versus the energy lost in the BGO calorimeter. The pattern corresponding to proton events is clearly visible in the $\Delta E_{\mathrm{barrel}}$ range between 4 and 20 MeV, whereas pion events cover

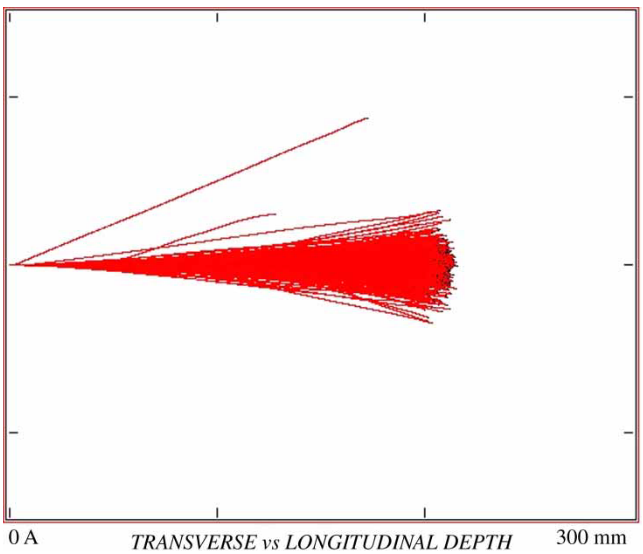

Figure 2. Output of the SRIM simulation: case in which the energy of the proton is 450 MeV. Each crystal of the BGO has a longitudinal length of 24 cm (color online).

Table 1. Percentage of transmitted protons at various energies is reported, according to the SRIM code.

Energy (MeV)	Transmitted (%)
300	0.0
400	0.0
450	0.0
480	0.0
490	20.3
495	67.2
500	94.0
510	99.1
520	99.6
530	100.0

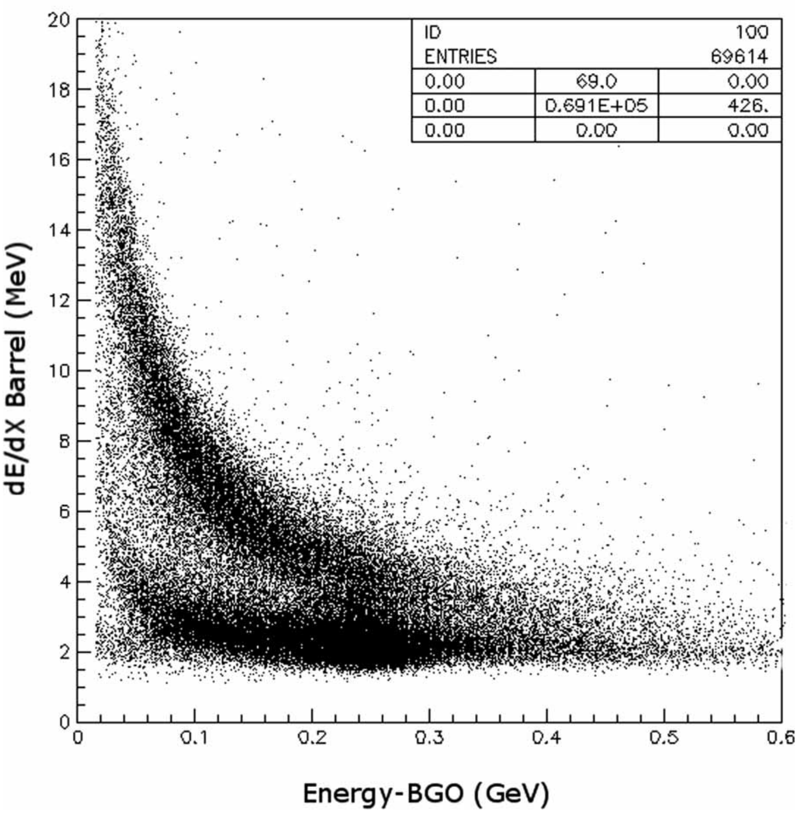

Figure 3. Energy lost in the barrel vs. energy lost in the BGO calorimeter.

the range from 1.5 to 3.5 MeV. By means of two polygonal lines (not shown in the figure), we have graphically identified protons and pions. The set of events to be analyzed has been selected by requiring the simultaneous detection of proton and charged pion.

The information obtained from the apparatus, which tags the incoming photon, provides a kinematical overdetermination of the event, so that energy or angles of one particle, directly measured in the detector, can also be calculated from variables of the other particle, using the two-body kinematics. In Figure 4 (left panel), the distribution of $\Delta\theta$ vs. $\Delta\varphi$ is shown; here, $\Delta\theta = \theta_{\text{miss,p}} - \theta_{\text{pion}}$, where $\theta_{\text{miss,p}}$ is the pion angle estimated from the proton kinematics and

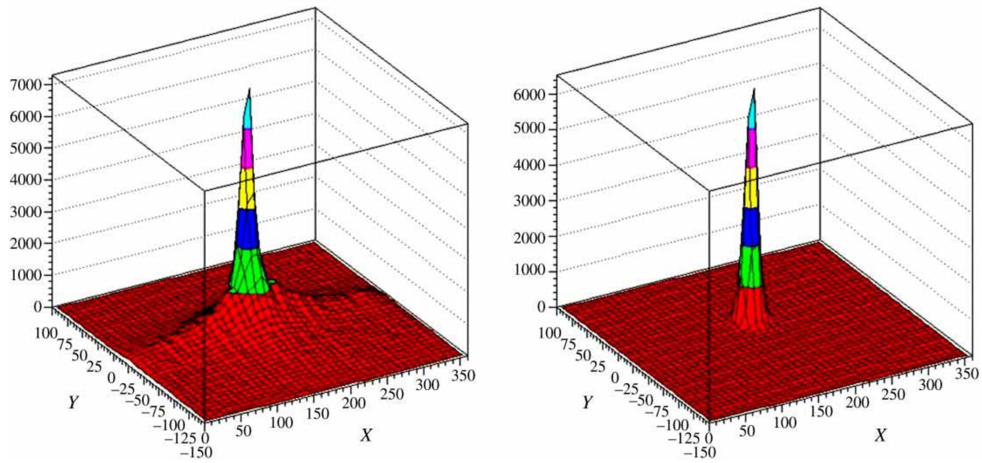

Figure 4. $\Delta\theta$ vs. $\Delta\varphi$ without (left panel) and with (right panel) Fermi momentum cut; in both cases, $\Delta\theta$ (Y-axis) and $\Delta\varphi$ (X-axis) have a value around 0° and 180°, respectively.

θ_{pion} is its measured value, whereas $\Delta\varphi$ is the difference between the azimuthal angles of the two particles. The accepted events are distributed (Figure 4, left panel) around $|\Delta\varphi| = 180°$, which identifies a two-event reaction final state.

In order to reduce the background contribution, we have performed an additional cut on the Fermi momentum (P_F) and, in particular, events with $P_F > 150$ MeV/c were rejected. In Figure 4 (right panel), the final selection is presented. The percentage of rejected events after such a cut is about 70%.

Finally, in Figure 5, a comparison between the measured and simulated energy for the proton and the pion (in coincidence with the pion and the proton, respectively) is shown. In both cases, the difference in energy is very close to zero, and the small asymmetry is probably due to hadronization effects, with the aforementioned incident gamma energies and solid angle covered by the BGO.

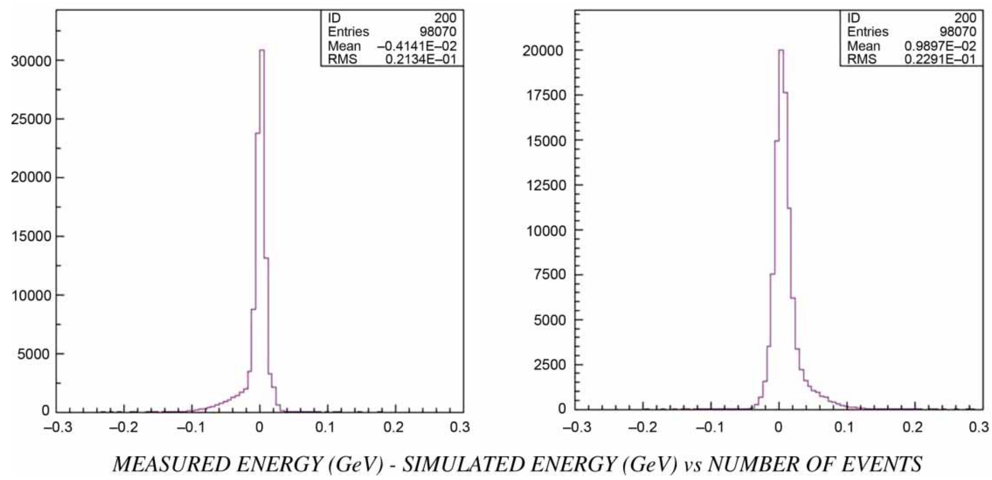

Figure 5. Difference between the measured and simulated energy for the proton (left panel) and pion (right panel).

4. Conclusions

In this paper, experimental results on the detection of both proton and pion using the GRAAL apparatus is presented. In particular, a direct measure of the energy was made by using the BGO calorimeter and the results obtained were compared with SRIM- and GEANT3-based simulations. A good agreement has been found between experimental and simulation data.

References

(1) Bartalini O.; Bellini V.; Bocquet J.P.; Capogni M.; Castoldi M.; D'Angelo A.; d'Angelo A.; Didelez J.P.; Di Salvo R.; Fantini A.; Gervino G.; Ghio F.; Girolami B.; Giusa A.; Guidal M.; Hourany E.; Kuznetsov V.; Lapik A.; Levi Sandri P.; Lleres A.; Moricciani D.; Nedorezov V.; Nicoletti L.; Randieri C.; Rebreyend D.; Renard F.; Rudnev N.V.; Schaerf C.; Sperduto M.L.; Sutera C.M.; Turinge A.; Zabrodin A.; Zucchiatti, A. *Nucl. Phys. A* **2002**, *699*, 218–225.

(2) Ziegler, J.F.; Biersack, J.P.; Littmark, U. *The Topping Power Range of Ions in Matter*; Ziegler, J., Ed.; Pergamon: New York, 1985.

(3) Bartalini, O.; Bellini, V.; Bocquet, J.P.; Capogni, M. ; Casano, L.; Castoldi, M.; Calvat, P.; Annalisa D'Angelo; Di Salvo, R. ; Fantini, A.; Gaulard, C.; Gervino, G.; Ghio, F.; Girolami, B.; Giusa, A.; Kuznetsov, V.; Lapik, A.; Levi Sandri, P.; Lleres, A.; Moricciani, D.; Mushkarenkov, A.N.; Nedorezov, V.; Nicoletti, L.; Perrin, C.; Rebreyend, D.; Renard, F.; Rudnev, N.; Russew, T.; Russo, G.; Schaerf, C.; Sperduto, M.L.; Sutera, M.C.; Turinge, A. *Eur. Phys. J. A* **2005**, *26*, 399–419.

(4) Schaerf, C. *Phys. Today* **2005**, *58*, 44–50.

(5) Ajaka, J.; Assafiri, Y.; Bartalini, O.; Bellini, V.; Bouchigny, S.; Castoldi, M.; D'Angelo, A.; Didelez, J.P.; Di Salvo, R.; Fantini, A.; Fichen, L.; Gervino, G.; Ghio, F.; Girolami, B.; Giusa, A.; Guidal, M.; Hourany, E.; Kunne, R.; Lapik, A.; Levi Sandri, P.; Moricciani, D.; Mushkarenkov, A.; Nedorezov, V.; Randieri, C.; Rudnev, N.; Russo, G.; Schaerf, C.; Sperduto, M.; Sutera, M.; Turinge, A. *Phys. Lett. B* **2007**, *651*, 108–113.

(6) Levi Sandri P.; Ghio F.; Moricciani D.; Breuer M.; Rigney M.; Didele J.P.; Djalali C.; Anghinolfi M.; Bianchi N.; Capogni M.; Casano L.; Corvisiero P.; D'Angelo A.; DeSanctis E.; DiSalvo R.; Gervino G.; Girolami B.; Hu L.; Muccifora V.; Polli E.; Reolon A.R.; Ricco G.; Ripani M.; Rossi P.; Sanzone M.; Schaerf C.; Taiuti M.; Zucchiatti A. *Nucl. Instrum. Methods Phys. Res. A* **1996**, *370*, 396–402.

(7) Ghio F.; Girolami B.; Capogni M.; Casano L.; Ciciani L.; D'Angelo A.; Di Salvo R.; Hu L.; Moricciani D.; Nicoletti L.; Nobili G.; Schaerf C.; Levi Sandri P.; Castoldi M.; Zucchiatti A.; Bellini V. *Nucl. Instrum. Methods Phys. Res. A* **1998**, *404*, 71–86.

(8) Castoldi M.; Di Salvo R.; Ghio F.; Girolami B.; Zucchiatti A.; Bellini V.; Capogni M.; Casano L.; Ciciani L.; D'Angelo A.; Gervino G.; Levi Sandri P.; Moricciani D.; Nicoletti L.; Rossi P.; Schaerf C. *Nucl. Instrum. Methods Phys. Res. A* **1998**, *403*, 22–30.

(9) Zucchiatti A.; Moricciani D.; Massone A.M.; Masulli F.; Capogni M.; Castoldi M.; D'Angelo A.; Ghio F.; Girolami B.; Levi Sandri P.; Sanzone, M. *Nucl. Instrum. Methods Phys. Res. A* **1999**, *425*, 536–548.

(10) GEANT, *Detector Description and Simulation Tool*, CERN Program Library Long Writeup.